

Contribution from the Department of Chemistry,  
Washington State University, Pullman, Washington 99164

## Electrochemistry of N-Heterocyclic Complexes of Rhodium(I) and Iridium(I)

W. A. FORDYCE, K. H. POOL, and G. A. CROSBY\*

Received June 15, 1981

Cyclic voltammograms and EPR spectra of stable reduced species are reported for some complexes of the general formula  $[M(\text{chel})(\text{diene})]^+$ :  $M = \text{Rh}(\text{I}), \text{Ir}(\text{I})$ ;  $\text{chel} = 2,2'$ -bipyridine, 1,10-phenanthroline, 4,7-diphenyl-1,10-phenanthroline, 2,2'-bipyrazine;  $\text{diene} = 1,5$ -cyclooctadiene, 2,5-norbornadiene. The complexes showed two reversible one-electron reductions in acetonitrile at a Pt wire electrode. EPR spectra of the one-electron-reduced species were typically singlets ( $\Delta H_{pp} \approx 8 \text{ G}$ ) at a  $g$  value of 2.001. The data indicate that the redox orbital is ligand  $\pi^*$ <sub>chel</sub>.

### Introduction

In the preceding article<sup>1</sup> we discussed the electronic spectroscopy of series of complexes of the general formula  $[M(\text{chel})(\text{diene})]^+$ .<sup>2</sup> We report here on the cyclic voltammetry of these complexes in acetonitrile and the EPR spectroscopy of stable reduced species.

Numerous investigators have examined the electrochemistry of complexes containing chelating N-heterocyclic ligands in nonaqueous solvents. Two recent reviews<sup>3,4</sup> discuss many of these reports. The majority of the studies have been concerned with complexes of first-row transition metals, Ru(II), and Os(II); DeArmond and co-workers<sup>5-11</sup> have conducted an extensive study of Rh(III) and Ir(III) complexes.

Electrochemical investigations of Rh(I) and Ir(I) complexes are less numerous. Dessy et al.<sup>12,13</sup> have published electrochemical data for several Rh(I) and Ir(I) species with  $\pi$ -bonded ligands. DeArmond and co-workers examined the electrochemistry of  $[\text{Rh}(\text{chel})_2]^+$  ( $\text{chel} = \text{bpy},^5 \text{phen}^6$ ) and the EPR spectra of electrochemically generated  $[\text{Rh}(\text{chel})_2]^{07}$  during the course of their study of Rh(III) complexes. Other complexes examined have contained primarily phosphine<sup>14-17</sup> and phosphite<sup>18</sup> ligands. Recently Sofranko et al. reexamined the electrochemistry of  $[\text{Rh}(\text{diphos})_2]^+$ <sup>19</sup> and described the

Table I. Cyclic Voltammetry Data<sup>a</sup>

complex	$E_{pc}$ (peak I) <sup>b</sup>	$E_{pc}$ (peak II) <sup>b</sup>
$[\text{Rh}(\text{bpy})(\text{cod})]\text{ClO}_4$	-1.26	-1.73
$[\text{Rh}(\text{phen})(\text{cod})]\text{ClO}_4$	-1.27	-1.74
$[\text{Rh}(4,7\text{-Ph}_2\text{-phen})(\text{cod})]\text{ClO}_4$	-1.23	-1.65
$[\text{Rh}(\text{bpz})(\text{cod})]\text{PF}_6 + \text{bpz}^c$	-0.75	-1.29
$[\text{Rh}(\text{bpy})(\text{nbd})]\text{ClO}_4$	-1.28	-1.76
$[\text{Rh}(\text{phen})(\text{nbd})]\text{ClO}_4$	-1.29	-1.76
$[\text{Ir}(\text{bpy})(\text{cod})]\text{ClO}_4$	-1.09 <sup>d</sup>	-1.55
$[\text{Ir}(\text{bpy})(\text{nbd})]\text{PF}_6$	-1.10	-1.57

<sup>a</sup> In 0.1 M TEAP in acetonitrile at a Pt wire, scan rate 50-500 mV/s. <sup>b</sup> Potential of cathodic peak in volts. <sup>c</sup> 1:10 molar ratio of complex to free ligand. <sup>d</sup> Weak adsorption peak at -0.96 V in anodic scan

electrocatalytic capabilities of  $[\text{Rh}(\text{diphos})_2]^{019,20}$  [ $\text{diphos} = 1,2$ -bis(diphenylphosphino)ethane].

Our goal was to characterize the redox orbital<sup>21</sup> (i.e., the orbital involved in the oxidation or reduction) of the complexes  $[M(\text{chel})(\text{diene})]^+$  and compare the results with the spectroscopic characterization of the acceptor orbital (i.e., the low-lying orbital involved in electronic excitation).<sup>1</sup> A previous report<sup>22</sup> of the electrochemistry of some of these complexes has been reinterpreted.

### Experimental Section

**Materials.** Ligand abbreviations are defined in ref 2. All complexes were prepared as described previously.<sup>1</sup> Electrolyte solutions for electrochemical measurements were prepared from acetonitrile distilled over  $\text{CaH}_2$ . Reagent grade  $[(\text{C}_2\text{H}_5)_4\text{N}]\text{ClO}_4$  (TEAP) was twice recrystallized from water and dried in vacuo over  $\text{P}_2\text{O}_5$ .

**Cyclic Voltammograms.** Cyclic voltammograms were obtained with use of a PAR Model 174A polarographic analyzer and a PAR Model RE0074 X-Y recorder. Scan rates ranged from 50 to 500 mV/s. The PAR Model 303 three-electrode cell consisted of a Ag/AgCl in 0.1 M tetraethylammonium chloride in acetonitrile reference electrode, a platinum wire auxiliary electrode, and a platinum wire working electrode. The Pt wire working electrode was preconditioned in degassed 0.1 M TEAP in acetonitrile electrolyte solution by scanning the accessible potential range several times before addition of sample. Voltammograms of all samples ( $\sim 10^{-3} \text{ M}$ ) were recorded in 0.1 M TEAP in acetonitrile degassed with acetonitrile-saturated nitrogen. Rather than compensate for  $iR$  drop, we compared  $\Delta E_p$  values with the  $\Delta E_p$  value of the ferrocene/ferrocenium couple under the same experimental conditions,<sup>23</sup> namely 70 mV. All potentials reported were corrected to the aqueous SCE reference with use of the reported potential of the ferrocene/ferrocenium couple (0.307 V vs. aqueous SCE).<sup>24</sup>

- (1) Fordyce, W. A.; Crosby, G. A. *Inorg. Chem.*, preceding paper in this issue.
- (2) Key to abbreviations used in this paper:  $M = \text{Rh}(\text{I}), \text{Ir}(\text{I})$ ;  $\text{chel} = \text{en}$  (ethylenediamine),  $\text{bpy}$  (2,2'-bipyridine),  $\text{phen}$  (1,10-phenanthroline), 4,7- $\text{Ph}_2$ - $\text{phen}$  (4,7-diphenyl-1,10-phenanthroline),  $\text{bpz}$  (2,2'-bipyrazine);  $\text{diene} = \text{cod}$  (1,5-cyclooctadiene),  $\text{nbd}$  (2,5-norbornadiene), 1,5-hex (1,5-hexadiene).
- (3) Budnikov, G. K.; Troepal'skaya, T. V. *Usp. Khim.* 1979, 48, 829.
- (4) Kapoor, R. C.; Kishan, J. *J. Sci. Ind. Res.* 1979, 38, 674.
- (5) Kew, G.; DeArmond, K.; Hanck, K. *J. Phys. Chem.* 1974, 78, 727.
- (6) Kew, G.; Hanck, K.; DeArmond, K. *J. Phys. Chem.* 1975, 79, 1828.
- (7) Caldararu, H.; DeArmond, M. K.; Hanck, K. W.; Sahini, V. E. *J. Am. Chem. Soc.* 1976, 98, 4455.
- (8) Hanck, K.; DeArmond, K.; Kew, G.; Kahl, J.; Caldararu, H. In "Characterization of Solutes in Non-Aqueous Solvents"; Mamantov, G., Ed.; Plenum Press: New York, 1977.
- (9) Kahl, J. L.; Hanck, K. W.; DeArmond, K. *J. Phys. Chem.* 1978, 82, 540.
- (10) Kahl, J. L.; Hanck, K. W.; DeArmond, K. *J. Phys. Chem.* 1979, 83, 2606.
- (11) Kahl, J. L.; Hanck, K. W.; DeArmond, K. *J. Phys. Chem.* 1979, 83, 2611.
- (12) Dessy, R. E.; Stary, F. E.; King, R. B.; Waldrop, M. *J. Am. Chem. Soc.* 1966, 88, 471.
- (13) Dessy, R. E.; King, R. B.; Waldrop, M. *J. Am. Chem. Soc.* 1966, 88, 5112.
- (14) Olson, D. C.; Keim, W. *Inorg. Chem.* 1969, 8, 2028.
- (15) Piloni, G.; Valcher, S.; Martelli, M. *J. Electroanal. Chem. Interfacial Electrochem.* 1973, 40, 63.
- (16) Piloni, G.; Vecchi, E.; Martelli, M. *J. Electroanal. Chem. Interfacial Electrochem.* 1973, 45, 483.
- (17) Piloni, G.; Martelli, M. *J. Electroanal. Chem. Interfacial Electrochem.* 1973, 47, 89.
- (18) Piloni, G.; Zotti, G.; Martelli, M. *J. Electroanal. Chem. Interfacial Electrochem.* 1975, 63, 424.
- (19) Sofranko, J. A.; Eisenberg, R.; Kampmeier, J. A. *J. Am. Chem. Soc.* 1979, 101, 1042.

- (20) Sofranko, J. A.; Eisenberg, R.; Kampmeier, J. A. *J. Am. Chem. Soc.* 1980, 102, 1163.
- (21) Vlcek, A. A. *Rev. Chim. Miner.* 1968, 5, 299.
- (22) Makrlík, E.; Hanzlík, J.; Camus, A.; Mestroni, G.; Zassinovich, G. *J. Organomet. Chem.* 1977, 142, 95.
- (23) Gagne, R. R.; Koval, C. A.; Linsensky, G. C. *Inorg. Chem.* 1980, 19, 2855.

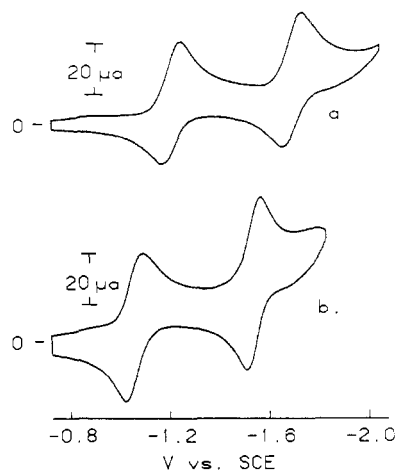


**Figure 1.** Cyclic voltammograms of (a)  $[\text{Rh}(\text{bpy})(\text{cod})]\text{ClO}_4$  and (b)  $[\text{Ir}(\text{bpy})(\text{nbd})]\text{PF}_6$  in 0.1 M TEAP in acetonitrile; scan rate 200 mV/s.

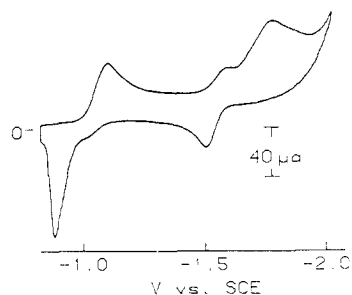


**Figure 2.** Cyclic voltammogram of  $[\text{Ir}(\text{phen})(\text{cod})]\text{ClO}_4$  in 0.1 M TEAP in acetonitrile; scan rate 200 mV/s.

**EPR Spectra.** EPR spectra were obtained on an X-band Varian E-3 spectrometer. Reduced complexes were prepared in situ in an electrolytic EPR cell commercially available from Wilmad Glass Co. The three electrodes were a reference electrode described above, a tungsten wire auxiliary electrode at the base of the cell hooked in parallel with a Pt auxiliary electrode at the top of the cell, and a Pt wire working electrode that extended into the EPR cavity region. The potential was controlled with the PAR Model 174A polarographic analyzer. Sample solutions were prepared and degassed as described above.

## Results

**Cyclic Voltammetry.** The cyclic voltammetry data are summarized in Table I. Electrooxidations at a Pt wire electrode gave poorly defined and irreproducible voltammogram peaks. (For studies of some of these complexes with a dropping mercury electrode at oxidizing potentials, see Makrlík et al.<sup>22</sup>) The diene = 1,5-hex complexes discussed in the previous paper<sup>1</sup> decomposed in acetonitrile, yielding complex voltammograms, and were not studied further. The chel = en complexes showed no reduction waves out to potentials as low as -2 V. For the complexes in Table I the potential separation between cathodic and anodic peaks was 70 mV and independent of scan rate. Therefore the  $E_{1/2}$  reduction potentials may be calculated by adding 35 mV to the potentials in Table I. In general the cathodic and anodic peak currents were equal except in the case of  $[\text{Rh}(\text{bpy})(\text{nbd})]\text{ClO}_4$ . For this complex the anodic peak current of the second reduction wave was significantly reduced.

The most striking feature in Table I is the relative insensitivity of the reduction potentials to changes both of diene and of chel (except bpz). Change of the metal center from Rh(I) to Ir(I) caused the reduction potential to shift  $\sim 0.2$  V. The separation between the first and second reduction po-

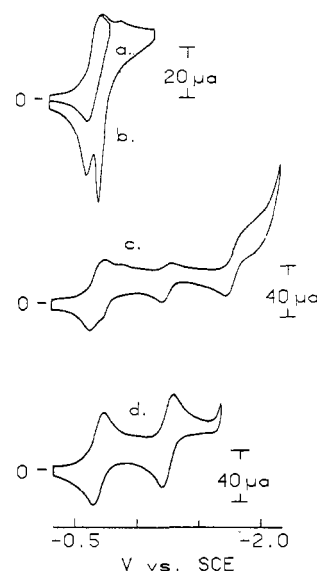


**Figure 3.** Cyclic voltammograms of (a-c)  $1.17 \times 10^{-3}$  M  $[\text{Rh}(\text{bpz})(\text{cod})]\text{PF}_6$  and (d)  $1.17 \times 10^{-3}$  M  $[\text{Rh}(\text{bpz})(\text{cod})]\text{PF}_6$  and  $1.17 \times 10^{-2}$  M bpz in 0.1 M TEAP in acetonitrile; scan rate 200 mV/s.

**Table II.** EPR Spectral Data

complex	g values	$\Delta H_{\text{pp}}$ , G <sup>a</sup>
$[\text{Rh}(\text{bpy})(\text{cod})]^0$	2.001	7.0
$[\text{Rh}(\text{phen})(\text{cod})]^0$	2.000	8.5
$[\text{Rh}(4,7\text{-Ph}_2\text{-phen})(\text{cod})]^0$	2.001	7.3
$[\text{Rh}(\text{bpz})(\text{cod})]^0$	2.001	12.0
$[\text{Rh}(\text{bpy})(\text{nbd})]^0$	2.001	21.1 <sup>b</sup>
$[\text{Rh}(\text{phen})(\text{nbd})]^0$	2.001	8.5
$[\text{Ir}(\text{bpy})(\text{cod})]^0$	2.001	9.0
$[\text{Ir}(\text{phen})(\text{cod})]^0$	2.001	9.5
$[\text{Ir}(\text{bpy})(\text{nbd})]^0$	2.001	8.5

<sup>a</sup> Peak to peak width; all spectra were singlets unless noted otherwise. <sup>b</sup> Total spectrum width; nine-line spectrum.

tentials was  $\sim 0.5$  V. Cyclic voltammograms of  $[\text{Rh}(\text{bpy})(\text{cod})]\text{ClO}_4$  and  $[\text{Ir}(\text{bpy})(\text{nbd})]\text{PF}_6$  are shown in Figure 1.

The cyclic voltammograms of  $[\text{Ir}(\text{phen})(\text{cod})]\text{ClO}_4$  (Figure 2) and  $[\text{Rh}(\text{bpz})(\text{cod})]\text{PF}_6$  (Figure 3) were considerably more complicated than the others.  $[\text{Ir}(\text{phen})(\text{cod})]\text{ClO}_4$  exhibited an intense postpeak after the second cathodic peak and a sharp spike at approximately -0.9 V on the reverse scan (Figure 2). Reversing the scan after the first cathodic peak increased the intensity of the anodic spike. Addition of excess phen did not significantly alter the voltammogram (vide infra). Scan reversal after the first cathodic peak of  $[\text{Rh}(\text{bpz})(\text{cod})]\text{PF}_6$  produced a normal anodic peak (Figure 3a). Continuation of the cathodic scan revealed a broad "plateau" feature and upon reversal a sharp anodic spike (Figure 3b). When the scan was continued out to -2 V, additional peaks at approximately -1.3 and -1.8 V and a reduction in the intensity of the anodic spike were observed (Figure 3c). The reduction at -1.8 V coincided with the reduction of free bpz. The addition of a tenfold excess of bpz to the solution gave the voltammogram shown in Figure 3d.

**EPR Spectra.** In situ electrolysis of electrolyte solution or solutions of free bpy ligand at potentials as low as -1.8 V produced no EPR signals. Electrolysis of complexes at the first reduction potential caused immediate grow-in of an EPR signal concurrent with formation of a deep blue species at the Pt working electrode. Slow formation of a black deposit on the Pt working electrode also accompanied the electrolysis of  $[\text{Rh}(\text{bpz})(\text{cod})]\text{PF}_6$  and  $[\text{Ir}(\text{phen})(\text{cod})]\text{ClO}_4$ . Spectra were obtained after several minutes of electrolysis time. The signal slowly diminished after electrolysis was stopped. In the case of the Rh(I) complexes in which the starting solutions were

(24) Bard, A. J.; Faulkner, L. R. "Electrochemical Methods"; Wiley: New York, 1980; p 701.

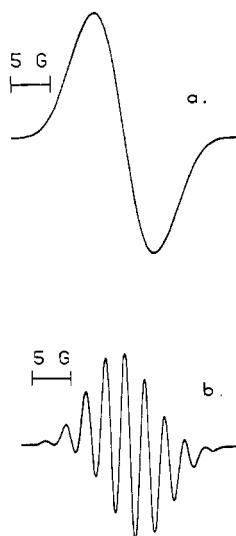


**Figure 4.** Room-temperature EPR spectra of (a)  $[\text{Rh}(\text{bpy})(\text{cod})]^{0}$  and (b)  $[\text{Rh}(\text{bpy})(\text{nbd})]^{0}$  in 0.1 M TEAP in acetonitrile.

air-stable, exposure of the blue electrolyzed solutions to air produced a change back to the original color. The EPR spectral data are summarized in Table II.

The EPR spectrum of  $[\text{Rh}(\text{bpy})(\text{cod})]^{0}$  shown in Figure 4a was typical of most of the complexes examined. Only the spectrum of  $[\text{Rh}(\text{bpy})(\text{nbd})]^{0}$  (Figure 4b) showed hyperfine structure, consisting of nine lines separated by 2.5 G. The EPR spectrum of the same complex at 77 K consisted of a single line similar to the other spectra.

#### Discussion

The 70-mV separation of cathodic and anodic peaks, in agreement with the value obtained for the reversible oxidation of ferrocene, and the equality of cathodic and anodic peak currents (independent of scan rate) lead us to conclude that each reduction peak represents a one-electron reversible process. The reduced current of the anodic peak for the second reduction of  $[\text{Rh}(\text{bpy})(\text{nbd})]^{+}$  is probably caused by slow decomposition (resulting in the loss of bpy) of the two-electron-reduced species,  $[\text{Rh}(\text{bpy})(\text{nbd})]^{-}$ , as suggested by Makrlik et al.<sup>22</sup>

We now focus attention on the redox orbital, i.e., the orbital involved in the reduction process. The tris complexes of Fe(II), Ru(II), and Os(II) with bpy and substituted bpy<sup>25</sup> and phen and substituted phen<sup>26</sup> show significant dependence of the reduction potential upon variations of chel. Consequently the redox orbital was characterized as predominately  $\pi^*_{\text{chel}}$ . The lack of a similar dependence for the complexes studied here, the absence of a dependence of the reduction potential upon variations of diene, and the dependence upon the metal led Makrlik et al.<sup>22</sup> to characterize the redox orbital as metal centered. In view of the results from the chel = en and bpz complexes that we have added to the series, the relationship of the electrochemical data with the spectroscopic data,<sup>1</sup> and the EPR data, we propose that the redox orbital is predominately  $\pi^*_{\text{chel}}$ .

By analogy with ligand field arguments for six-coordinate complexes<sup>27</sup> we would not expect the metal orbitals to be significantly shifted upon substitution of ethylenediamine for the N-heterocycle. Therefore, if the redox orbitals were metal centered, the reduction potentials should only be slightly al-

tered; yet, we observed no reduction waves at all for the en complexes. This argues in favor of a  $\pi^*_{\text{chel}}$  (except chel = en) redox orbital.

Correlations between the reduction potentials of the free ligands and those of the complexes have been found for the Fe(II), Ru(II), and Os(II) tris complexes with N-heterocyclic ligands.<sup>25,26</sup> Although the reduction potentials of the complexes studied here are relatively insensitive to chel, the reversible reductions of  $[\text{Rh}(\text{bpz})(\text{cod})]\text{PF}_6$  in the presence of excess bpz (vide infra) are substantially shifted to lower reducing potentials. This is consistent with the lower reduction potential of bpz (-1.8 V) relative to bpy (-2.10 V)<sup>25</sup> and phen (-1.99 V).<sup>26</sup>

Saji and Aoyagui have also found a correlation between the oxidation potentials of the Fe(II), Ru(II), and Os(II) tris complexes<sup>28</sup> and the energies of their low-lying charge-transfer absorptions. For the complexes studied here we find a similar trend with the reduction potentials. The low-lying charge-transfer transitions are relatively insensitive to variations of chel,<sup>1</sup> as are the reduction potentials, except when chel = bpz. For  $[\text{Rh}(\text{bpz})(\text{cod})]\text{PF}_6$  the low-lying charge-transfer absorption is significantly red shifted,<sup>1</sup> and the reduction potential is decreased relative to the other complexes. The same trend holds when Rh(I) is replaced with Ir(I).

Although the reduction potentials of the free ligands would be expected to change considerably upon coordination, the potential difference between the first and second ligand reductions should not change substantially. Although reports differ,<sup>25,26,29</sup> values for the potential gap between successive reductions of bpy<sup>25</sup> and phen<sup>29</sup> of ~0.5 V have been reported. This is the same value found for the complexes studied here and for the  $\text{Zn}(\text{chel})(\text{R})_2$  (chel = bpy, phen; R = C<sub>2</sub>H<sub>5</sub>, C<sub>6</sub>H<sub>5</sub>) complexes examined by El-Shazly.<sup>30</sup>

The complex cyclic voltammograms of  $[\text{Ir}(\text{phen})(\text{cod})]\text{ClO}_4$  (Figure 2) and  $[\text{Rh}(\text{bpz})(\text{cod})]\text{PF}_6$  (Figure 3) are dominated by adsorption processes.<sup>31</sup> DeArmond and co-workers have observed electrode adsorption of  $[\text{M}(\text{phen})_2]^{0}$  [M = Rh(I),<sup>6</sup> Ir(I)<sup>10,11</sup>] species and postulated a phen ring interaction by examining the analogous iridium complex containing the sterically hindered 5,6-Me<sub>2</sub>-phen ligand. We have not studied these processes in detail, but some general statements can be made. In both complexes the zerovalent species,  $[\text{M}(\text{chel})(\text{diene})]^{0}$ , is adsorbed on the electrode surface in agreement with DeArmond's results.<sup>6,10,11</sup> The sharp anodic spikes after the first reduction are a result of oxidative desorption of the adsorbed species. The intense feature following the second reduction wave of  $[\text{Ir}(\text{phen})(\text{cod})]\text{ClO}_4$  may correspond to reduction and desorption of the adsorbed species. As discussed previously<sup>6</sup> the presence of well-defined desorption peaks, yet the absence of adsorption peaks at the same potential, suggests that the models for adsorption developed by Shain and co-workers are not applicable to these species.<sup>31</sup>

The first reversible reduction of  $[\text{Rh}(\text{bpz})(\text{cod})]\text{PF}_6$  is apparently followed by an adsorption process (causing the "plateau feature") producing the desorption spike on the anodic scan. The second reduction of the complex appears at approximately -1.3 V, and the reduction of free bpz, probably liberated by decomposition of reduced species, appears at -1.8 V. Upon addition of a tenfold excess of bpz these adsorption processes are eliminated. The resulting voltammogram (Figure 3d) shows two reversible reductions and the reduction of bpz (not shown in the figure). The mechanism of this adsorption

(25) Saji, T.; Aoyagui, S. *J. Electroanal. Chem. Interfacial Electrochem.* **1975**, *58*, 401.

(26) Musumeci, S.; Rizzarelli, E.; Fragala, I.; Sammartano, S.; Bonomo, R. P. *Inorg. Chim. Acta* **1973**, *7*, 660.

(27) Basolo, F.; Pearson, R. G. "Mechanisms of Inorganic Reactions"; Wiley: New York, 1967; p 67.

(28) Saji, T.; Aoyagui, S. *J. Electroanal. Chem. Interfacial Electrochem.* **1975**, *60*, 1.

(29) Dessy, R. E.; Charkoudian, J. C.; Rheingold, A. L. *J. Am. Chem. Soc.* **1972**, *94*, 738.

(30) El-Shazly, M. F. *Inorg. Chim. Acta* **1978**, *26*, 173.

(31) (a) Wopschall, R. H.; Shain, I. *Anal. Chem.* **1967**, *39*, 1514. (b) Hulbert, M. H.; Shain, I. *Ibid.* **1970**, *42*, 162.

inhibition is not clear. Cyclic voltammograms of bpz show no adsorption effects, indicating either that bpz does not compete with the complex for adsorption or that adsorbed bpz is not electroactive.

Tanaka et al.<sup>32</sup> have examined the EPR spectra of electrochemically generated  $[\text{Fe}(\text{bpy})_3]^+$  and  $\text{bpy}^-$ . They report single-line ( $\Delta H_{\text{pp}} = 97$  and  $7.5$  G, respectively) EPR spectra at  $g = 1.995$  and  $2.004$ , respectively. The EPR spectra of the one-electron-reduced species examined here (except  $[\text{Rh}(\text{bpy})(\text{nbd})]^0$ ) greatly resemble that of  $\text{bpy}^-$ . The  $g$  values, spectral widths (Table II), and absence of  $^{103}\text{Rh}$  hyperfine splittings [in the case of the Rh(I) complexes] indicate that the  $\pi^*_{\text{chel}}$  redox orbital contains no metal character. Although symmetry allows  $(n+1)p_z$  character in the  $\pi^*_{\text{chel}}$  acceptor orbital of the complexes, we concluded that the amount was quite small.<sup>1</sup> Thus we assert that *both the acceptor and the redox orbitals can be characterized as  $\pi^*_{\text{chel}}$* . The EPR spectra obtained here differ radically from the EPR spectra of  $[\text{Rh}(\text{chel})_2]^0$  (chel = bpy, phen).<sup>7</sup> Steric hindrance of the chel ligands forces a distorted planar geometry in the bis complexes<sup>33</sup> and would probably result in a different electronic structure.

Although hyperfine structure is generally absent in our and Tanaka's spectra in acetonitrile, EPR spectra of complexes containing N-heterocyclic ligands recorded at room temperature in 1,2-dimethoxyethane usually show structure.<sup>29,30,34</sup> The only hyperfine structure we observed was contained in the EPR spectrum of  $[\text{Rh}(\text{bpy})(\text{nbd})]^0$ . An excellent computer simulation was possible by employing the following coupling constants:  $a_{\text{NN}'} = 2.5$  G,  $a_{4\text{H}^8} = 2.5$  G (line width = 3 G).<sup>35</sup> We make no attempt to assign the positions of the four hydrogens.

Several other workers have reported EPR spectra of the bpy anion radical or of complexes containing bpy that exhibit hyperfine structure. Veiga et al.<sup>36</sup> analyzed the EPR spectrum of the bpy anion radical. Their hyperfine coupling constants differ from ours as would be expected from changes in the  $\pi$  electronic structure of the ligand upon coordination with an electron-rich metal center. Our EPR spectrum of  $[\text{Rh}(\text{bpy})(\text{nbd})]^0$  is nearly identical with that of reduced  $\text{Zn}(\text{phen})(\text{C}_6\text{H}_5)_2$  reported by El-Shazly.<sup>30</sup> His simulation, which is identical with the simulation reported by Dessy et al.<sup>29</sup> for the phen anion radical, fits the number of lines and line widths

(which rules out line modulation effects) but does not fit the line intensities. We believe this simulation is in error. Dessy et al.<sup>34</sup> have reported that the EPR spectrum of reduced  $\text{Mo}(\text{bpy})(\text{CO})_4$  gives hyperfine coupling constants in agreement with those observed for reduced bpy, but no spectra are shown.

Also of interest is the similarity of the  $[\text{Rh}(\text{bpy})(\text{nbd})]^0$  EPR spectrum to that of  $[\text{Cr}(\text{bpy})_3]^+$  (ignoring the  $^{53}\text{Cr}$  hyperfine lines) reported by König.<sup>37</sup> The  $^{52}\text{Cr}$  portion of the spectrum clearly contains at least nine lines, but the tails are obscured by hyperfine lines from the  $^{53}\text{Cr}$  satellites. König concluded that the  $^{52}\text{Cr}$  portion of the spectrum contained 13 lines (6 nitrogens). The similarity of the  $[\text{Rh}(\text{bpy})(\text{nbd})]^0$  EPR spectrum (2 nitrogens) may shed new light on his analysis.

The apparent identity of the EPR signals of the one- and two-electron-reduced species suggests that  $[\text{M}(\text{chel})(\text{cod})]^-$  reacts with  $[\text{M}(\text{chel})(\text{cod})]^+$  in solution to form  $[\text{M}(\text{chel})(\text{cod})]^0$ . We infer that the second reduction corresponds to pairing of the added electrons on chel, forming diamagnetic  $[\text{M}(\text{chel})(\text{cod})]^-$ . This hypothesis was tested with  $[\text{Rh}(\text{bpy})(\text{cod})]\text{ClO}_4$  in the following manner. Electrolysis for 1 min at either the one- or the two-electron reduction potential produced EPR signals of equal intensity, yet electrolysis at the one-electron reduction potential for 1 min followed immediately by electrolysis at the two-electron reduction potential for 1 min produced a significantly weaker EPR signal. In the second experiment the electrode was bathed in  $[\text{Rh}(\text{bpy})(\text{cod})]^0$ , inhibiting reaction of  $[\text{Rh}(\text{bpy})(\text{cod})]^-$  with bulk solution  $[\text{Rh}(\text{bpy})(\text{cod})]^+$ .

The stability of the  $[\text{M}(\text{chel})(\text{diene})]^0$  species is in sharp contrast to the highly reactive species produced by the reduction of  $[\text{Rh}(\text{diphos})_2]^+$ .<sup>19,20</sup> The difference may lie in the increased ability of the  $\pi$  aromatic system of the chel ligand to accept electron density.

**Acknowledgment.** This research was supported by Air Force Office of Scientific Research Grant AFOSR-80-0038. We are also grateful to Professor D. X. West for helpful discussions concerning the EPR results and computer simulations. We thank Matthey Bishop, Inc., for a generous loan of rhodium and iridium chlorides.

**Registry No.**  $[\text{Rh}(\text{bpy})(\text{cod})]\text{ClO}_4$ , 37685-01-1;  $[\text{Rh}(\text{phen})(\text{cod})]\text{ClO}_4$ , 37685-03-3;  $[\text{Rh}(4,7\text{-Ph}_2\text{-phen})(\text{cod})]\text{ClO}_4$ , 80263-16-7;  $[\text{Rh}(\text{bpz})(\text{cod})]\text{PF}_6$ , 80263-18-9;  $[\text{Rh}(\text{bpy})(\text{nbd})]\text{ClO}_4$ , 52445-04-2;  $[\text{Rh}(\text{phen})(\text{nbd})]\text{ClO}_4$ , 52445-07-5;  $[\text{Ir}(\text{bpy})(\text{cod})]\text{ClO}_4$ , 41444-85-3;  $[\text{Ir}(\text{bpy})(\text{nbd})]\text{PF}_6$ , 53505-25-2;  $[\text{Rh}(\text{bpy})(\text{cod})]^0$ , 80263-19-0;  $[\text{Rh}(\text{phen})(\text{cod})]^0$ , 80263-20-3;  $[\text{Rh}(4,7\text{-Ph}_2\text{-phen})(\text{cod})]^0$ , 80263-27-0;  $[\text{Rh}(\text{bpz})(\text{cod})]^0$ , 80263-21-4;  $[\text{Rh}(\text{bpy})(\text{nbd})]^0$ , 80263-22-5;  $[\text{Rh}(\text{phen})(\text{nbd})]^0$ , 80263-23-6;  $[\text{Ir}(\text{bpy})(\text{cod})]^0$ , 80263-24-7;  $[\text{Ir}(\text{phen})(\text{cod})]^0$ , 80263-25-8;  $[\text{Ir}(\text{bpy})(\text{nbd})]^0$ , 80263-26-9.

(32) Tanaka, N.; Ogata, T.; Niizuma, S. *Bull. Chem. Soc. Jpn.* **1973**, *46*, 3299.

(33) McKenzie, E. D. *Coord. Chem. Rev.* **1971**, *6*, 187.

(34) Dessy, R. E.; Wiczorek, L. *J. Am. Chem. Soc.* **1969**, *91*, 4963.

(35) The hyperfine line intensities are 0.8:5.5:16.2:30.5:36 ...; our simulation yields 1:6:17:30:36 ... If we assume eight equivalent hydrogens,  $a = 2.5$  G, the predicted line intensities are 1:8:28:56:70 ...

(36) Veiga, J. Dos Santos; Reynolds, W. L.; Bolton, J. R. *J. Chem. Phys.* **1966**, *44*, 2214.

(37) König, E. *Z. Naturforsch., A* **1964**, *19A*, 1139.